Proceedings of the Twenty-third (2013) International Offshore and Polar Engineering **www.isope.org**
Anchorage, Alaska, USA, June 30–July 5, 2013

ISBN 978-1-880653-99–9 (Set); ISSN 1098-6189 (Set)

Structural Behaviour of High-Frequency-Induction (HFI) Welded Line Pipe Subject to External Loads

Susanne Höhler
Salzgitter Mannesmann Forschung GmbH
Duisburg, Germany

Holger Brauer
Salzgitter Mannesmann Line Pipe GmbH
Hamm, Germany

ABSTRACT

This paper addresses bending actions and curvature on pipelines that may occur accidentally due to external loads or ground movements for buried pipelines. The scenario is characterized by extreme plastic deformations where tensile straining and stability issues (buckling) need to be considered. The structural pipe behaviour is estimated via analytic equations in an isotropic manner using von Mises plasticity. Analytically, limit values for bending actions or plastic strains are derived. The analyses are supported by a full-scale test on a pressurized HFI welded pipe of steel grade X70, accompanied by material testing, from which strain hardening properties were derived.

KEY WORDS:

Full-scale test; HFI-pipes; modelling; compression; bending; buckling; multiaxial stress-strain;

NOMENCLATURE

A_5	elongation at break
A_g	uniform elongation
C_H	constant (Hollomon)
F	von Mises yield surface
$k(\varepsilon_v^p)$	function of the plastic strain
OD	outer diameter
R_m	tensile strength
$R_{p0.2}$	tensile yield strength at 0.2% plastic strain
$SMYS$	specified minimum yield strength
t	wall thickness
Y/T	ratio of $R_{p0.2}/R_m$
$d\lambda$	plastic multiplier; Lagrange multiplier
n_H	strain hardening exponent (Hollomon)
ε	strain
ε_{ave}	average strain
ε_v^p	equivalent plastic strain
σ	stress
$\sigma_{d3.0}$	compression strength at 3.0 % strain
$\sigma_{d0.2}$	compression yield strength at 0.2 % strain

INTRODUCTION

The conventional approach for pipeline design is a stress-based approach. The hoop stress in the pipe wall is limited by a design factor on the specified minimum yield strength (SMYS). This approach leaves open the question for the actual safety factor for some specific failure cases. The stress-based engineering approach may be insufficient for displacement-controlled or partly displacement-controlled load scenarios, such as pipeline deformations due to ground movement or thermal effects. In order to meet the increasing safety demands by assuring integrity of new pipelines of modern steels even in a terrain with challenging soil conditions, alternative strain-based design methods should be introduced for cases where ground movements may play a role.

Strain-based scenarios have in common that large plastic strains can develop in the pipe wall. As regards ground movements axial strains from curvatures or bending forces must be considered in addition to circumferential elongation due to internal pressure from the transport of the medium. The assessment of the structural safety of such pipelines under combined loading requires the knowledge of the plastic response of line pipe. The plastic deformation capacity depends on the pipe dimensions, loading and notably the strain hardening behaviour. If axial strains are compressive, e.g. in the compressive fiber of the pipe section due to curvature or a bending moment, then moreover local deformations such as buckles need to be controlled which are largely steered by the pipe geometry.

The complexity of strain-based design increases with the variety of newly developed pipe steels and pipe manufacturing processes, where experience from the past is not available. Reliable predictive models are needed that have been validated by experimental data. In testing, it is important that a realistic scenario is simulated using a full-scale pipe

specimen in order to comprehend the structural performance. If the constitutive properties are assessed on material level, without full-scale data, essential information of the multiaxial pipe behaviour will be missing, for example strain redistribution, residual stresses or imperfections. The following sections elaborate on a full-scale test performed on a pressurized pipe under bending load and on the analytic modelling for predicting the structural behaviour via certain assumptions.

FULL-SCALE-TESTING

The SZMF testing device

The test rig located at Salzgitter Mannesmann Forschung GmbH (SZMF) in Duisburg, Germany, is a vertical four-point-bending device. It is equipped with four hydraulic jacks with each 2500 kN (two cylinders act on one load application point, respectively). Thus, a total load capacity of 10 000 kN (1000 tons) can be supplied. The bearings are supported by a welded steel frame. An overview of the test rig is sketched in **Figure 1**.

Maximum width between supports is about 15.5 m; diameters may reach up to 56" and steel grades may go up to API 5L X100. The hydraulic jacks allow for a maximum stroke of 1100 mm. One of the outer bearings is undisplaceably fixed to the steel frame while the other bearing and the two loading planes can be moved flexibly along the pipe axis, see **Figure 2**. Thus, the pipe length and the distance between the supports can be chosen according to the pipe dimensions and test requirements. If a pressurized pipe is bent the internal pressure is achieved by water filling. For this purpose the pipe ends are sealed via end caps welded onto them.

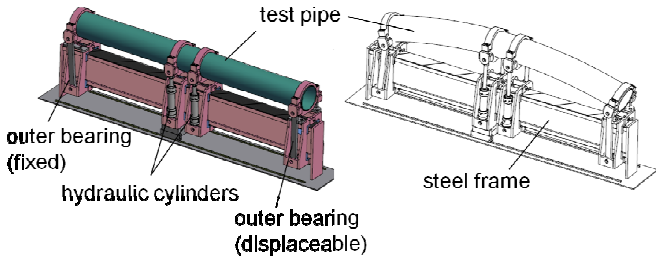

Figure 1: Full-scale bending test rig at SZMF

Test pipe X70, 24"

The test has been performed on a HFI pipe produced by Salzgitter Mannesmann Line Pipe GmbH in API X70 steel grade and 24" diameter (OD x t: 609.6 x 10 mm). In order to include any thermal aging effects from the polymer-coating process, where the pipe temperature can reach 200°C - 250°C for several minutes, the test pipe had undergone a heat treatment as if being provided with poly-ethylene (PE)-coating. In fact the test pipe was heated for 5 minutes with the temperature of 210°C. Thus, a realistic application of a poly-ethylene (PE)-coated pipe was simulated.

To achieve an overview of the mechanical properties tensile and compressive material tests were carried out taking into account different hoop positions of the pipe cross section. Both longitudinal and hoop direction were tested in order to identify possible anisotropic material behaviour. **Table 1** presents the tensile material data; **Table 2** contains the compressive test results.

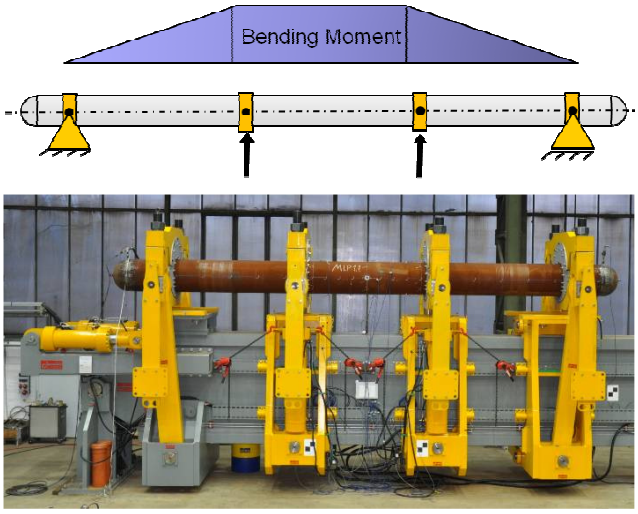

Figure 2: Schematic and photo of four-point bending test at SZMF

Table 1: Tensile test results (mean values from two single tests; samples: long.: flat specimens with width 25mm, transverse: round bar B5x25, not flattened, DIN 50125)

Clock position, orientation		$R_{p0.2}$ MPa	R_m MPa	Y/T -	A_g %	A_5 %
3°°	Long.	509	609	0.84	13.3	27.5
6°°	Long.	510	609	0.84	13.1	27.3
6°°	Transv.	497	625	0.80	13.3	28.3
9°°	Long.	508	608	0.84	12.9	27.0

Table 2: Compressive test results (mean values from two single tests; cylindrical samples Ø 8mm, height 16mm, extracted from exterior of pipe wall)

Clock position, orientation		$\sigma_{d0.2}$ MPa	$\sigma_{d3.0}$ MPa	$\sigma_{d0.2}/\sigma_{d3.0}$ -
3°°	Long.	518	599	0.86
6°°	Long.	512	615	0.83
6°°	Transv.	534	634	0.84
9°°	Long.	518	603	0.86

The test pipe was installed in the test rig such that the 3°° o`clock fibre was positioned in the extrados and so the 9°° o`clock position in the intrados. The HFI weld was located in the neutral bending axis. The pipe was instrumented with strain gauges and trip wire displacement sensors in three measuring planes (planes A, B, C) within the test section, see **Figure 3**.

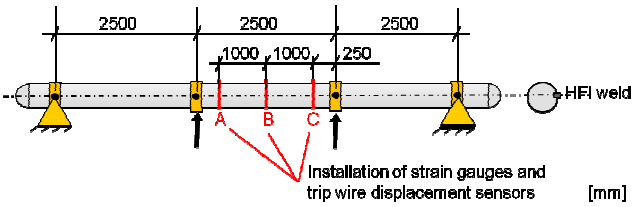

Figure 3: Schematic of test pipe installation and instrumentation

The test has been carried out in displacement controlled condition. The internal pressure level of 66% SMYS was selected (corresponding to a hoop stress equal to 66% of SMYS) which lead to a pressure of 100 bar. The pressurization had been completed before bending and pressure was kept constant throughout the bending test.

Test results

After reaching the load maximum buckling appeared. The test was continued into the post-buckling regime where load decrease was observed, but after a certain cylinder stroke (500 mm) the test was discontinued and the pipe unloaded. As usual for pressurized pipes, buckling occurred in form of characteristic outward bulges. In this case, two bulges developed symmetrically to the pipe mid-length section (**Figure 4**, **Figure 5**).

Figure 4: Pipe deformation after test; close-up view of test section

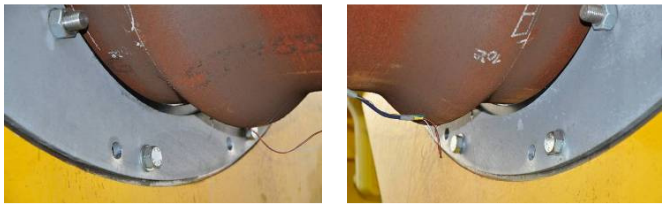

Figure 5: Close-up view of bulges

Figure 6 presents the load-deflection curve which is an average curve of the left and right jacks' forces and strokes recorded during the test. Strain measurements from strain gauges are reported in **Figure 7** and **Figure 8**. The strains in plane A and plane C (Figure 7) indicate a symmetric behaviour of the pipe related to mid-length section, as plane A and plane C show almost identical curves, both on the tensile and the compressive fibre. Strain records in plane B (Figure 8) are supplemented by transverse direction.

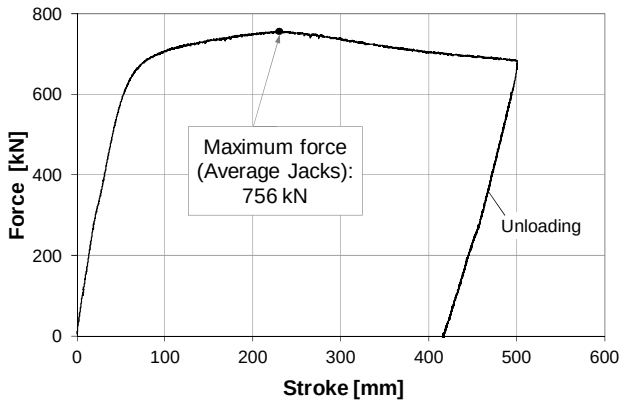

Figure 6: Load-deflection diagram (average of left and right jacks)

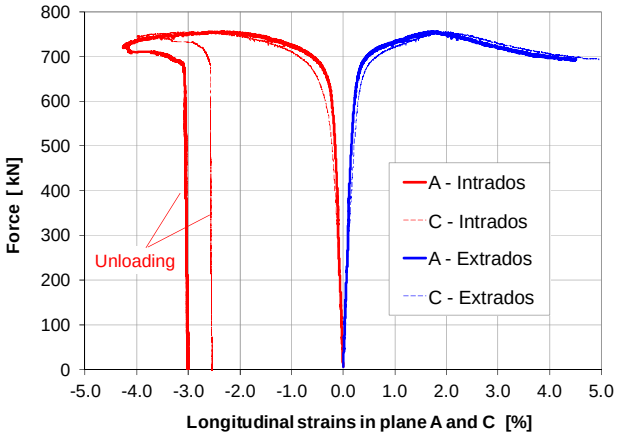

Figure 7: Load-strain curves in measurement planes A, C acc. Figure 3

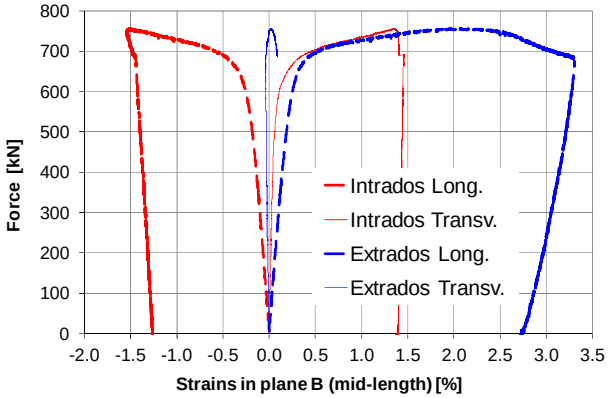

Figure 8: Strains in plane B (mid-pipe length section acc. to Figure 3)

Figure 8 reveals different load-strain curves for the extrados and intrados. For one thing the pipe behaviour differs for compressive and tensile loading, which already became clear when looking at the material tests where compressive and tensile data differ slightly. Secondly, due to the influence of the internal pressure, the pipe did not deform symmetrically towards the neutral bending axis.

The strains measured in the neutral bending axis, in 90° angle with respect to intrados and extrados, are not depicted in this paper. They were close to zero with marginal deviations, as expected for this load case.

Figure 7 and Figure 8 point out very similar longitudinal strains recorded on the extrados, in all three planes A, B and C. In contrast, on the intrados, higher strains are observed in planes A and C in comparison to plane B (mid section). Measurement planes A and C are near the loading planes, and next to planes A and C the bulges developed as a consequence of the higher strains. The load devices may have contributed to this behaviour by introducing local deformation into the pipe wall. In addition, the relatively high pipe pressure may have had an influence. Other test series have shown that highly pressurized pipes tend to shift the bulges towards the loading planes, while pipes with lower or zero pressure buckled in mid section. The quantification of these effects will be studied in current and further research work.

ANALYTIC PREDICTION OF PIPE BEHAVIOUR

Analytic formulation of three-dimensional plastic straining

An analytic model to predict multi-axial stress and strain states in pipelines subject to external axial forces and bending loads has been developed. The general format of the assessment procedure was already published in [Höhler et al., 2009; Höhler and Brauer, 2011]. Basically, the von Mises yield criterion is applied, where the yield surface (F) includes the stress state as well as the strain hardening parameter $k(\varepsilon_v^p)$. Yielding occurs if the yield condition is met, see Eq. (1):

$$F = \sqrt{\sigma_\phi^2 + \sigma_x^2 + \sigma_r^2 - \sigma_\phi\sigma_x - \sigma_x\sigma_r - \sigma_r\sigma_\phi} - k\left(\varepsilon_v^p\right) = 0 \quad (1)$$

The stresses in the pipe wall in transverse, axial and radial co-ordinate direction (σ_ϕ, σ_x, σ_r) are principal stresses. The strain hardening behaviour is introduced as a function of the plastic strains $k(\varepsilon_v^p)$. The stress-strain results derived from uniaxial tensile or compression tests are considered, starting from yield strength and ending at tensile strength by reaching the uniform elongation. In case of compression tests the stress-strain results between 0.2 % and 3.0 % plastic strains are used. Tensile as well as compressive stress-strain curves are approximated by a function of the plastic strains $k(\varepsilon_v^p)$ where a function following Hollomon power law [Hollomon, 1949] represents the curve's shape in a realistic manner:

$$k(\varepsilon_v^{\ p}) = C_H \cdot \left(\varepsilon_v^{\ p}\right)^{n_H} \quad (2)$$

In Eq. (2) n_H is the Hollomon strain hardening exponent and C_H is a material constant. These parameters are determined e.g. through a curve fitting process via Eq. (2).

Using the strain components in all three pipe co-ordinate directions (ε_ϕ, ε_x, ε_r) the von Mises equivalent plastic strain is formulated as:

$$\varepsilon_v^p = \sqrt{\frac{2}{3}\varepsilon_{ij}^p\varepsilon_{ij}^p} = \sqrt{\frac{2}{3}}\sqrt{\left(\varepsilon_\phi^p\right)^2 + \left(\varepsilon_x^p\right)^2 + \left(\varepsilon_r^p\right)^2} \quad (3)$$

Next to yielding, consistency must be met, assuring that any load increase from a plastically deformed state will result in another plastically deformed state. The consistency condition (4) ensures for every incrementally increased stress state again a fulfilled yield condition:

$$dF = 0 \quad (4)$$

Respecting Eq. (4) and knowing the stress state in the pipe wall as well as the strain hardening function, Eq. (1) and Eq. (2), the plastic strain contributions can be calculated incrementally in all three directions. The stress-strain relationship for isotropic hardening materials is considered. The plastic strain increments then read:

$$d\varepsilon_{ij} = d\lambda\frac{\partial F}{\partial\sigma_{ij}} \quad (5)$$

Here $d\varepsilon_{ij}$ is the plastic strain tensor normal to yield surface. The term $\partial F / \partial\sigma_{ij}$ is called the flow rule. It describes the partial derivative of the yield surface F with respect to the components of the stress tensor σ_{ij} and defines in which direction plastic flow will take place. $d\lambda$ is the plastic or "Lagrange" multiplier, which has to be determined for any subsequent plastic loading. It can be directly evaluated by reformulating the consistency condition, Eq. (4), which is the total derivative of Eq. (1).

Model application on bending test on pressurized HFI pipe

The limit states related to tensile straining can be assessed with the methods described above. However, in case of bending moment both tensile and compressive strains develop in the pipe section. Then stability mechanisms, such as buckling most likely dominate structural pipe behaviour. The full-scale test presented here confirmed this, since even for high pressure utilization the development of bulges was the first failure mechanism to occur. Yet, depending on pipe geometry (ratio of diameter to wall-thickness OD/t) and the possible presence of girth welds in the test section, this may not always be the case. For an analytic approach both aspects, tensile straining and buckling, must be addressed. Literature and codes provide a variety of formulae to deter-

mine buckling loads or critical compressive strains. Comparing different theoretical modelling approaches it was shown, that the DNV-OS-F101 [DNV-OS-F101] provides a suitable assessment of critical buckling strains for line pipe when exposed to axial forces, bending moment and internal pressure [Karbasian et al., 2012].

The analytic calculation was carried out stepwise, namely:

1. The critical buckling strain for the compressive zone of the bent pipe section was calculated via the procedure given in [DNV-OS-F101]. The material data used are compressive data gained from the 9°° o`clock position in longitudinal direction (Table 2), as the 9°° o`clock position corresponded the intrados in the bending test.

2. The stress-strain evolution until the buckling strain is reached and the corresponding limit bending moment (and bending force) came from the analytic calculation described in the equations above. The same compressive material data was inserted as in step 1. The underlying stress-strain curve was used to determine the strain hardening exponent n_H and Hollomon constant C_H.

3. The stress-strain evolution for the tensile zone of pipe section was calculated via the analytic equations using tensile test material data, again using n_H and Hollomon constant C_H. The material data from 3°° o`clock position in longitudinal direction (Table 1) was applied as the 3°° o`clock pipe position was placed in the extrados position in the bending test.

Figure 9 shows the load-strain evolution determined for the compressive zone in comparison to the test graphs recorded in planes A, B and C according to Figure 3. In the diagram total strains are plotted (including elastic and plastic deformation) in axial pipe direction. A circle in the calculated curve marks the critical buckling state: The buckling strain of 2.0 % has been estimated via [DNV-OS-F101]. The corresponding force was F = 730 kN.

From Figure 9 it can be concluded that the critical buckling strain of 2.0 % seems to have been predicted in a realistic magnitude which is confirmed by the strain graphs measured in the three measuring planes A, B and C. The strains in the test corresponding to the load maxima were:

plane A $\varepsilon = 2.32$ %,
plane B: $\varepsilon = 1.52$ %
plane C: $\varepsilon = 2.77$ %

The calculation considers a uniform deformation within the pipe section of constant bending stress. However, in the test, buckling occurred much closer to plane A and plane C than to plane B (mid-length). The critical buckling strain is the compressive strain right before buckling takes place. Commonly, the critical compressive strain is not regarded as one locally measured value, but defined as the average compressive strain over a defined gauge length, see for example [Shitamoto et.al., 2012]. Here the critical average compressive strain in the test pipe section is assessed as the average of the three measurement planes (ε_{ave} = 2.2 %).

The load-strain evolution for the tensile pipe fiber is additionally presented in **Figure 10**. The strain measurements from pipe extrados and the calculated curve are included.

The load–strain evolution for both the compressive and the tensile zone of the pipe show higher strains and thus lower forces in the calculation compared to the test measurements, see also Figure 10. The calculated force-strain curves leave the elastic path once the elastic bending moment has been exceeded, steered by the yield strength ($R_{p0.2}$ and $\sigma_{d0.2}$, respectively) gained in the material tests. The actual structure showed a much stiffer and less "round-house shape" behaviour. The elastic path is continued to higher bending forces before the pipe showed significant plastic deformations. As a consequence the predicted buckling force (730 kN) is 3.5 % lower than the measured load maximum (756 kN).

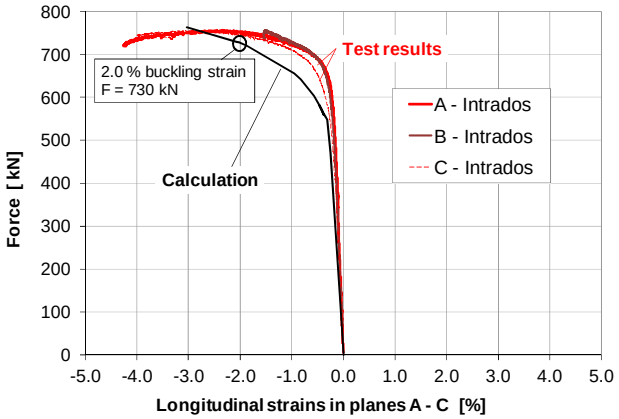

Figure 9: Load-strain evolution for the compressive zone

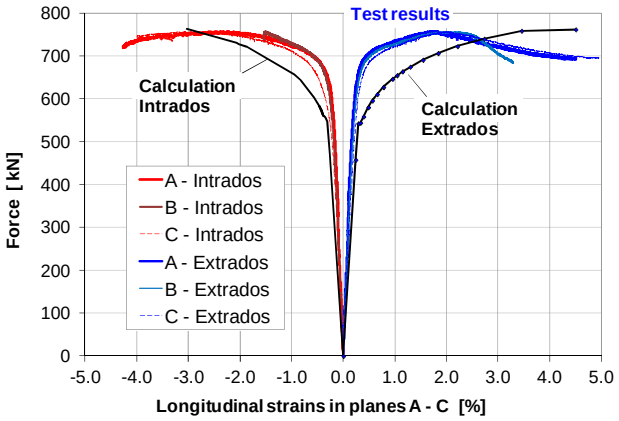

Figure 10: Load-strain evolution for compressive and tensile zone

The deviation of test and analyses proves once more that the complex structural performance of a pipe under such a multiaxial load case cannot be described by simple uniaxial material tests or material parameters anymore. [Brauer et al., 2007] made similar observations on ring expansion tests. Even the here applied three-dimensional analytical model represents the structural pipe behaviour only with a certain inaccuracy. An important reason for the deviation is the material anisotropy which has not been considered in the analytical model. The calculations are, in the present case, completely based on longitudinal material data (tensile and compressive), where anisotropy of longitudinal versus hoop direction is not included. Yet, it is known that PE coated HFI pipes show a greater anisotropy than "as rolled" pipes [Brauer et.al., 2013]. In such a multiaxial load case with high pressure loading, the transverse behaviour influences the pipe performance considerably.

The significance of anisotropy is furthermore revealed in **Figure 11** and **Figure 12**. Next to the strains in longitudinal direction the transverse strains are added, of test as well as calculation. The test results are from strain gauges, the calculated curves are based on longitudinal material data. Figure 11 contains the graphs for the intrados, Figure 12 for the extrados. Here, also the calculated strains deviate from the test measurements, which most likely is due to material anisotropy not yet implemented in the analytic modelling procedure.

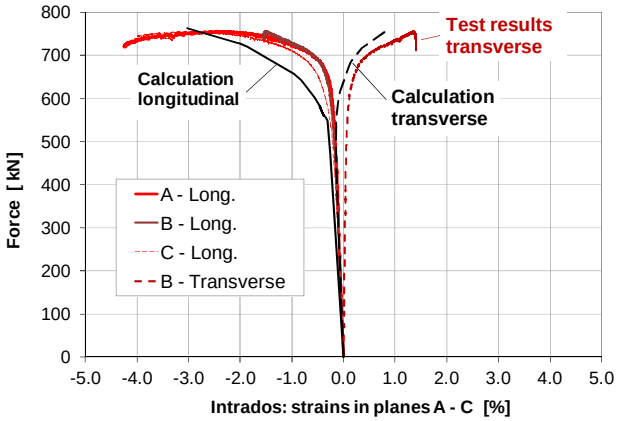

Figure 11: Load–strain evolution for intrados: longitudinal and transversal strains

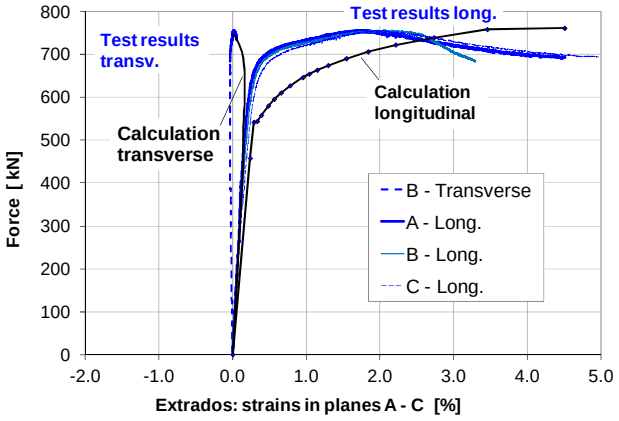

Figure 12: Load–strain evolution for extrados: longitudinal and transversal strains

CONCLUSIONS

The structural behaviour of a High-Frequency-Induction (HFI) welded pipe subject to bending loads was investigated via a full-scale bending test and analytic predictions. The investigations provide a further step to support the development of suitable strain-based design concepts. In the experiment the pressurized pipe showed typical buckling behaviour by developing outward bulges. The load-deflection curves and strain measurements reflected the typical buckling phenomenon.

The calculations based on the von Mises yield criterion and isotropic strain hardening material reveal the complexity of pipe behaviour in terms of anisotropy. Anisotropic material properties need to be considered in further modelling as well as pipe imperfections to reproduce the elastic plastic deformation behaviour more accurately. Approaches for the implementation of anisotropy into analytical and FE calculations have been treated by [Hilgert et al., 2012] where extended von Mises plasticity is applied using Hill parameters.

Next to the consideration of anisotropy and imperfections future tests should aim at the comprehension of weld behaviour under bending loads. Girth welded pipe sections on the one hand will show a different plastic straining behaviour compared to a plain pipe. On the other hand the orientation of the longitudinal weld (HFI weld) may play a role, if placed on the extrados or intrados in the bending test.

REFERENCES

Brauer, H.; Löbbe, H.; Krägeloh, J.: Mechanical properties of HFI-welded pipes for linepipe under high operating pressures – Comparison of ring expansion test and tensile tests. 3R international 46 (2007) 4, pp. 213/6

Brauer, H.; Höhler, S.; Löbbe, H.: Influence of strain aging on parameters for assessment of multi-axial load histories of High-Frequency-Induction (HFI) welded line pipe, Proc ISOPE-2013. Anchorage, Vol 4

DIN 50125, 2009-07: Testing of metallic materials - Tensile test pieces

DNV-OS-F101, 2012-08: Offshore Standard - Submarine Pipeline Systems

Hilgert, O.; Zimmermann, S.; Kalwa, C.: Anisotropy – Benefits for UOE Line Pipe. *Proceedings of the 9th International Pipeline Conference 2012 (IPC2012)*, Calgary, Alberta, Canada

Höhler, S.; Zimmermann, S.; Brauer, H.; Löbbe, H.: Work hardening properties of High-Frequency-Induction (HFI) welded line pipe. *Proceedings of the 5th International Pipeline Technology Conference 2009*, Ostend, Belgium.

Höhler, S.; Brauer, H.: Resistance of HFI line pipe to external loads. 3R International, Journal 1/2011 Special Edition, pp 34/7.

Hollomon, J.H.: Tensile deformation. Transactions of the Metallurgical Society of the American Institute of Mining, Metallurgical and Petroleum Engineers (AIME) 16, 1949, pp 268/90

Karbasian, H.; Zimmermann, S.; Marewski, U.; Steiner, M.: Combined Loading Capacity of Pipelines - Approaches Towards the Compressive Strain Limit. *Proceedings of the 9th International Pipeline Conference 2012*, Calgary, Alberta, Canada

Shitamoto, H., Hamada, M., Takahashi, N., Nishi, Y.: Effect of Full Scale Pipe Bending Test Method on Deformability results of SAW Pipes. *Proceedings of the 22nd International Offshore and Polar Engineering Conference*, Rhodes, Greece, ISOPE, Vol 4, www.isope.org.